Scholar Publishing Group
International Journal of Sports Technology
https://doi.org/ 10.38007/IJST.2020.010101
ISSN 2789-7141 Vol. 1, Issue 1: 1-17

Dynamic Biomechanical Knee Joint Minute Flexion and Extension Sports

Minchang Li*

Department of Physical Education, Huazhong Agricultural University, Wuhan, Hubei, 430070, China

**corresponding author*

Keywords: Knee Joint, Tibiofemoral Joint, Micro-Flexion and Extension Exercise, Dynamic Biomechanics

Abstract: The knee joint plays an extremely important role in people's daily life, but it is often easy to cause injury. Therefore, under different sports conditions, the related changes in the muscles around the knee joint, and the changes have an effect on the movement of the knee joint and even the lower limbs. What kind of effect has become a hot topic of current research? The knee joint is the most complex in the structure of the human body. It is closely related to the human's exercise ability. It mainly realizes the movement of the human body by flexion and extension. The development level of most sports events is also restricted by the working ability and efficiency of the knee joint. The ability of the muscle group has a very important influence on its overall athletic ability. In this paper, the dynamic biomechanical analysis of the knee joint's micro-flexion and extension exercises is carried out, and positive preventive measures are taken reasonably to minimize the occurrence and the degree of injury. In this paper, medical image processing software mimics and finite element analysis software abaqus are used to construct three-dimensional finite element models of natural knee joints and artificial knee joints. The two finite element models are used to dynamically simulate the micro flexion and extension of the knee joint to study and analyze the knee joint in the flexion and extension state. Next, the biomechanical characteristics of the tibiofemoral joint and the relative motion between the joints. Experiments have shown that a compression force of 1200N is applied and an internal rotation torque of 8Nm is used. It is measured that the range of internal rotation of the knee joint is 2.25°to 29.34°and the range of external rotation is 1.75°to 33.34 during knee flexion from 0°to 60°. It can be seen that the angles of internal and external rotation gradually increase with the increase of flexion and extension, but the range of external rotation is slightly larger than the range of internal rotation. This is of great significance to the analysis of the biomechanics and movement of the Chinese natural knee joint and the artificial knee joint. It can better guide the design and optimization of the Chinese prosthesis; improve the matching degree of the prosthesis and the knee joint, and the postoperative prosthesis time of use.

1. Introduction

Human biomechanics is based on human physiology and anatomy, using mechanical principles and methods to study the structure, function, and motion laws of human organs. The research on knee joint biomechanics has attracted the attention of experts in biomechanics, clinical medicine and rehabilitation engineering. The knee joint is the pivot of the lower limbs of the human body, and its geometric structure and physiological movement are the most complicated of all joints. The finite element method has become a relatively mature and effective method of calculation and analysis, and is widely used in actual engineering. With the rapid development of science and technology, it has also been successfully applied to medical engineering and biomechanics, especially in orthopedics related to joint biomechanics. The finite element method showed significant advantages in the research. By studying the biomechanical properties of the knee joint during exercise, the stress distribution law and relative movement of the knee joint can be obtained, and then the mechanism of knee joint disease can be analyzed; for the prevention of knee joint sports injury, treatment and rehabilitation of knee joint disease and the design and optimization of artificial knee joint prostheses are of great significance.

With the rapid development and progress of science and technology, foreign countries have gradually penetrated the finite element method into various fields of practical engineering, including the field of biology. Because the finite element method can effectively analyze the stress characteristics of irregular geometric structures, making it widely used in many fields related to human body structure. Mika J combined the CT and MRI scan data of the knee joint to establish a relatively complete and ideal three-dimensional finite element model of the knee joint, which provides an effective tool for knee joint motion simulation and mechanical analysis [1]. Pame M assumed that there is a center of rotation between the inner and outer condyles of the femur of the knee joint, successfully simulated the gait motion of the knee joint, and analyzed the stress characteristics of the knee joint during the gait cycle [2]. Hoekstra M created a three-dimensional finite element model of total knee replacement, taking into account the contact friction between the articular surfaces and the constraints of soft tissues. And by controlling the force and moment to analyze the motion and contact stress of the artificial joint, and compare with the knee joint simulator test results to verify the validity of the model [3].

Compared with foreign countries, domestic research on finite element modeling of knee joints started late and relatively few, and there is a certain gap with foreign research. With the rapid development of science and technology in my country and the increasing importance of people’s health. More and more domestic scholars have begun to study knee biomechanics, and they are constantly narrowing the gap with foreign countries. Tseng F J established a relatively complete three-dimensional model of the knee joint, and set a constant muscle force, and then studied the changes in the contact stress between the joints and the force of the cruciate ligament under different flexion and extension angles [4]. Skvortsov DV has established a knee joint dynamics model that includes bones and muscles. It uses the interaction of ligament tension and muscle force to achieve knee joint movement. It studies and analyzes the influence of different muscle groups on knee joint movement, but this is a two-dimensional model [5]. Prlkov-Pukov A established a finite element model of the dynamic contact and wear of the tibial prosthesis. This model can apply axial loads, medial and lateral forces, and rotational torque to the knee joint, and can simulate gait and tibial prosthesis wear and material creep during the process of climbing stairs [6].

At present, there are not many domestic researches on muscle strength test and surface EMG change synchronization test, especially the research reports related to eccentric motion. At the same time, based on the three-dimensional geometric anatomical model of the natural knee joint, according to the knee replacement surgery according to the specification, a three-dimensional finite element model of the human natural knee joint including the bone tissues of the patella, femur and tibia, articular cartilage, meniscus, ligament and other major soft tissues should be established. Therefore, this paper adopts the analysis of muscle strength changes and surface electromyography during isokinetic motion. The combined analysis method is used to study and analyze the strength and electromyography of the flexor and extensor muscle groups at different muscle contractions and working speeds of the knee joint.

2. Dynamic Biomechanical Knee Joint Minute Flexion and Extension

2.1. Human Knee Joint Structure

(1) The structure and function of bone tissue

The knee joint is composed of the patella, the distal end of the femur and the proximal end of the tibia. It is the joint with the most complex structure and the largest amount of movement in the human body. Judging from the classification of joint types, the knee joint is a typical synovial joint [7]. The patella and the femoral trochlear constitute the patellofemoral joint; the internal and external condyles of the femur and the tibial plateau together constitute the tibiofemoral joint.

(2) Structure and function of soft tissue

1) Articular cartilage

Articular cartilage is a white transparent tissue with a thickness of 1-6mm wrapped on the surface of the joint. Its surface is smooth and adheres to a certain amount of synovial fluid. Articular cartilage does not contain blood vessels, lymphocytes, and related nerves. It is mainly composed of chondrocytes and intercellular substance. Cartilage cells are distributed in articular cartilage discretely, and their volume is less than the total volume of tissue. 10% of it is sparsely distributed, but chondrocytes have an indispensable role [8-9]. Articular cartilage has the following functions: articular cartilage has viscoelasticity, so during knee joint movement, it can increase the contact area, thereby equalizing pressure, reducing impact and absorbing shock; articular cartilage has synovial fluid attached to the surface, so it can the knee joint has a lubricating effect during movement and can reduce the relative friction between the joints.

2) Meniscus

The meniscus plays a key role in the movement of the knee joint: the surface of the knee joint is not very consistent, and the meniscus can fill the joint gap, and has a shock absorption function, which can improve the stability of the knee joint; the meniscus has a bearing and transmission function. It can also increase the contact area between the tibiofemoral joints to reduce the contact stress of the articular cartilage; the meniscus can release synovial fluid and help lubricate the joint movement [10].

3) Knee ligaments

When the knee is slightly flexed, there will be a certain amount of internal and external rotation. During this process, the medial and lateral collateral ligaments are easily injured, and the injured location is mostly around the attachment point of the ligament and the femoral condyle. In addition, the laxity of the lateral collateral ligament will also cause proper varus of the knee joint; and when the knee is excessively varus, it will cause damage to the lateral collateral ligament, and the general injury location is at the attachment of the ligament and fibula [11-12]. The cruciate ligament plays an important role in maintaining the stability of the knee joint; it can not only prevent excessive translation and rotation between the tibiofemoral joints, but also limit the excessive extension of the knee joint.

(3) Biomechanical properties of the knee joint

The load on the knee joint will vary significantly due to different sports. Since the meniscus and articular cartilage are both viscoelastic materials, they will deform when subjected to force, which will increase the contact area of the femur and tibia, thereby reducing the contact stress between the tibiofemoral joints. The stability of the knee joint depends on the special shape of the bone structure of the knee joint, the anterior and posterior cruciate ligaments, the medial and lateral collateral ligaments, the joint action and control of the knee extension device and the quadriceps femoris [13-14]. The tibia will have a certain external rotation relative to the femur, so the tibiofemoral joint will be in a locked state, so that the knee joint maintains the best stability; and when the knee joint is in a state of hyperflexion and extension, it will pass through the joint of the articular surface and the mutual restriction of the medial and lateral collateral ligaments and the anterior and posterior cruciate ligaments maintain the stability of the knee joint.

(4) Three-dimensional movement of the knee joint

The movement of the knee joint is caused by the joint action of bones and ligaments. The main movement is the tibiofemoral joint movement, while the main movement of the tibial joint is the flexion and extension of the sagittal plane of the human body. There are both relative rolling and relative sliding between them, so the center of rotation is constantly changing. Within 0 ° to 20 ° of flexion and extension, the tibiofemoral joint mainly rolls, and when the angle of flexion and extension is greater than 20 °, the tibiofemoral joint mainly slides [15-16]. In people's lives, the range of flexion and extension of the knee joint during walking is 5 ° to 70 °, and the maximum flexion and extension angle of the knee joint can reach 80 ° to 100 ° during the process of going up and down the stairs. When we do sports, the range of flexion and extension of the knee joint will become larger, and the form of motion of the knee joint will be more complicated.

2.2. Construction of Knee Joint Finite Element Model

(1) Finite element modeling of natural knee joint

In this paper, a CT scan of volunteer knee joints was performed. From the perspective of biomechanics, a normal knee including patella, femur, tibia and femur, articular cartilage, meniscus, and major ligaments of the knee joint was constructed through software such as mimics, HyperMesh, and abaqus. Three-dimensional finite element model of joints. The main process of constructing the natural knee joint finite element model is shown in Figure 1.

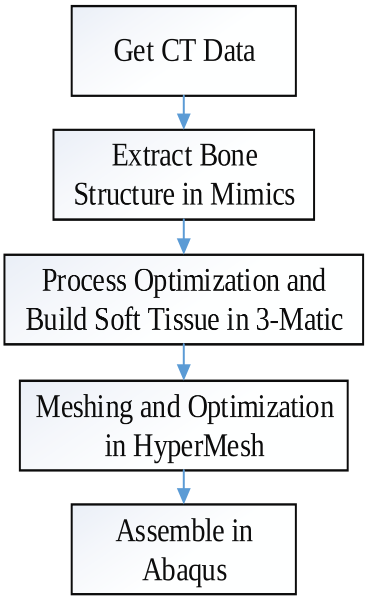

Figure 1. Flow chart of finite element model construction of natural knee joint

(2) Finite element modeling of artificial knee joint

When the knee joint exercises, the patella cartilage, femoral cartilage and tibial cartilage can reduce the direct friction between bones. However, when the knee joint suffers from lesions and injuries, the articular cartilage will be aging and damaged, which will increase the friction between the bones, which will cause pain and distortion of the knee joint and make people's daily life inconvenient [17-18].

1) Geometric model of artificial knee joint prosthesis

Artificial total knee arthroplasty has high requirements on the force line of the lower limbs. If the force line of the lower limbs is successfully reconstructed and the gap during flexion and extension is adjusted, the wear rate and survival rate of the tibial pad component will be significantly improved. Too little bone cutting can lead to limited knee flexion and pain in the front of the knee joint, too much bone cutting can cause patella fracture, and asymmetric bone cutting can make the patella unstable [19-20]. Therefore, in patella replacement, it is very important to perform symmetrical bone cutting, measure the thickness of the patella, and accurately restore the original thickness of the patella after replacement.

2) Meshing of knee joint prosthesis and construction of TKA finite element model

The definition of the boundary conditions of the femur and tibia is the same as that of the natural knee joint finite element model. Then the prosthesis is contacted with the corresponding bone respectively, and the femoral prosthesis and tibial cushion components are used for surface-to-surface contact with the penalty function. The body is the main surface, the tibial pad component is the slave surface, and the friction coefficient is 0.04. And define the corresponding area where contact may occur [21].

2.3. Two-phase Medium Model Based on Mixture Theory

(1) Based on porous media model

Volume fraction is a very important concept in porous media theory, expressed as the ratio of the volume of a certain component in the mixture to the total volume of the mixture. The distribution of each physical quantity can be described by the concept of volume fraction. The entire space range of the porous medium is occupied by the solid phase medium and the liquid phase medium at the same time. These two media occupy corresponding spaces. The size of this space can be expressed by volume fraction. Representation, and then the way to determine the volume fraction can be described by mixture theory.

Assume that the total volume of the porous medium is V, and the occupied space area is B.The medium is composed of k components, the volume V_a of a certain component $a(a=1,2,\Lambda,k)$ becomes part of the volume, At time t, any space point x is simultaneously occupied by k components of material point X_a. Suppose the volume fraction is:

$$\phi_a = \phi_a(x,t) \tag{1}$$

In the formula, x represents the material vector of the space point, and x is occupied by the particles of all k components at the same time. Part of the volume in the spatial domain B is expressed as:

$$V_a = \int_B \phi_a dV \tag{2}$$

$$dV_a = \phi_a dV \tag{3}$$

Therefore, the total volume can be expressed as:

$$V = \int_B dV = \sum_{a=1}^{k} V_a = \int_B \sum_{a=1}^{k} dV_a = \int_B \sum_{a=1}^{k} \phi_a dV \tag{4}$$

Under saturation conditions:

$$\sum_{a=1}^{k} \phi_a = 1 \tag{5}$$

(2) Under saturation conditions:

The mixture theory, based on the theory of continuum mechanics, is considered to be the theory of heterogeneous multiphase media with interactions inside objects in a three-dimensional space. The various components in the mixture maintain an independent state of movement, and each component fills the entire internal space.

1) Conservation of mass

Mass is a physical quantity that reflects the inertia of an object. For a substance with a volume of V, the initial time t_0 is taken as the reference time, and the total mass at time t is:

$$M = \int_V \rho(x,t) dv \tag{6}$$

Where $\rho(x,t)$ is the mass density related to time and location? According to the law of conservation of mass, the total mass of matter in any volume V does not change, that is, the matter derivative of M is zero:

$$\frac{dM}{dt} = 0 \tag{7}$$

Bringing the mass formula into the law of conservation of mass, using the matter derivative formula of volume integral, we get:

$$\frac{d}{dt}\int_V \rho(x,t) dv = \int_V \left[\frac{\partial \rho}{\partial t} + \nabla \cdot (\rho v) \right] dv = 0 \tag{8}$$

Since the above formula holds for any volume, the integrand is zero, and we get:

$$\frac{\partial \rho}{\partial t} + \nabla \cdot (\rho v) = 0 \tag{9}$$

Which is:

$$\frac{\partial \rho}{\partial t} + \rho \nabla \cdot v = 0 \tag{10}$$

This is the law of conservation of mass in the differential form of the space description method, that is, the continuity equation. From the quasi-incompressibility of articular cartilage, it can be seen that the density remains unchanged during the deformation process, so:

$$\frac{d\rho}{dt} = 0 \tag{11}$$

Obtained by the law of conservation of mass:

$$\rho\nabla\cdot v=0 \tag{12}$$

Therefore, it can be concluded that the divergence of the velocity field with incompressible cartilage is equal to zero.

2) Law of conservation of momentum

The law of conservation of momentum is that the time rate of change of the total momentum of an object is equal to the resultant force of all external forces acting on the object:

$$\frac{d}{dt}\int_V \rho v dv = F(total) \tag{13}$$

Where v represents the speed of any particle in the object, $F(total)$ is the resultant force of external forces, Generally, it includes physical strength f and face strength t. Any configuration from the initial time t_0 to the current time t, The volume of the object changes from V to v. At any mass point, the momentum of the volume element is $\rho v dv$, The total momentum of the object at time t is $\int_V \rho v dv$.

$$\frac{d}{dt}\int_V \rho v dv = \int_v \rho f dv + \oint_s t_n da \tag{14}$$

Using the reciprocal formula of volume integral and Formula 9 to get:

$$\frac{d}{dt}\int_V \rho v dv = \int_v \rho a dv \tag{15}$$

For the local form of the momentum conservation equation, using Gauss's theorem:

$$\oint_s t_n da = \int_v \nabla\cdot t dv \tag{16}$$

Bringing Formula 14 and Formula 15 to Formula 13, we get:

$$\int_v [\nabla\cdot t + \rho(f-a)] dv = 0 \tag{17}$$

When the above formula is true for the volume of any part of the object, the integrand is zero, and the momentum conservation equation in the differential form of the space description method is obtained:

$$\nabla\cdot t + \rho(f-a) = 0 \tag{18}$$

(3) Nonlinear hyperelastic model

The determination of the properties of cartilage materials has become a major focus in cartilage research. In mechanical analysis, there are two important material properties including elastic material properties and tissue permeability. Since hyperelastic materials have a strain energy function related to deformation, in this study we used the model proposed by Homles to establish a nonlinear hyperelastic model of articular cartilage. This model is represented by the Helmholtz strain energy function, namely:

$$\Psi = a_0 \frac{e^{a_1(I_1-3)+a_2(I_2-3)}}{I_3^{\beta}} \tag{19}$$

Where:

$$I_1 = trace(C) \tag{20}$$

$$I_2 = \frac{1}{2}\left(I_1^2 - trace\left(C^2\right)\right) \tag{21}$$

$$I_3 = \det(C) \tag{22}$$

Here: C is the right Cauchy-Green strain tensor, a_0、a_1、a_3、a_4、β is the relevant material mechanics parameter, and I_1、I_2、I_3 is the first, second and third principal invariants of C respectively.

3. Design of Dynamic Biomechanics Experiment of Knee Joint Slight Flexion and Extension

3.1. Knee Joint Model Construction

Use mimics to extract the three-dimensional model of the knee joint bones, and then import the generated knee joint bone tissue geometry model into 3-matic, and use the smooth and warp functions to smooth the surface of the patella, femur and tibia and optimize the wrapping. As well as the mark and offset functions to construct patella cartilage, femoral cartilage, tibial cartilage, and meniscus, respectively, to construct an ideal knee joint geometry model. Then use hyperMesh to mesh it, and finally use abaqus to define ligaments, material properties and boundary conditions to construct a finite element model of the natural knee joint; then use the specifications of total knee replacement to install the joint prosthesis on the knee on the joint, a finite element model of the artificial knee joint is constructed. Make full preparations for the smooth progress of the subsequent simulation. The model construction flowchart is shown in Figure 2.

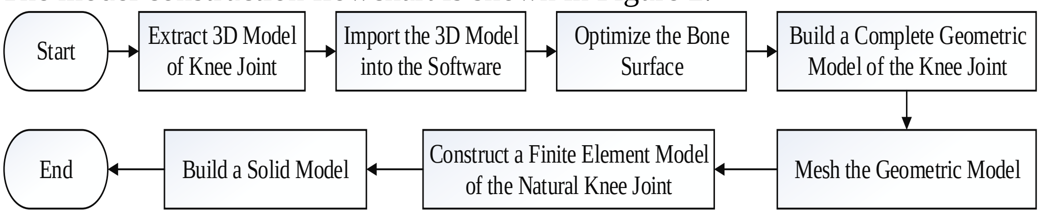

Figure 2. Knee joint model construction flowchart

3.2. Test Subject

To verify the accuracy of the model, load the model as follows: apply a rotational displacement load to the femur to dynamically simulate the 0 ° to 60 ° flexion and extension process of the knee joint. The rotation axis is the connection between the inner and outer condyle centers of the femur, which has limited three dimensions for the knee joint. The metamodel applies three different loads. Apply a compressive force of 1200N to the top section of the femur; apply a 150N femoral posterior thrust to the femur, and load it at the midpoint of the line connecting the midpoints of the inner and outer condyles of the femur; apply a compressive force of 1200N again to the knee joint apply 15Nm of varus and valgus moments to simulate knee joint movement of varus and valgus;

finally apply a compression force of 1200N, and apply 8Nm of internal and external rotation moments to the knee joint to simulate knee joint movement of internal and external rotation; group experiments get these experimental data, and comprehensively analyze these data to get the experimental results.

3.3. Experimental Method

According to the solution method of the nonlinear system balance equation established above, the finite element program is compiled, and the pseudo-static behavior of articular cartilage is analyzed through numerical simulation. The calculation process of the model is realized by C language programming in the VS environment. In the calculation process, the unit matrix of the data is used as the basic unit. The grid unit number and unit node coordinates have been extracted, so the geometric stiffness matrix and initial stress the matrix can be determined, and then the corresponding external load and boundary conditions need to be set, and the relationship between stress and velocity is calculated through the finite element program, and the model can be verified by obtaining the relevant stress-strain relationship.

4. Dynamic Biomechanical Experimental Knee Joint Micro-flexion and Extension

4.1. Evaluation Index System Based on Index Reliability Testing

Reliability represents the stability and trust of the questionnaire survey. This article analyzes the reliability of each object type. Although the reliability indicators of these object types will have subtle differences, the results are shown in Table 1:

Table 1. Summary table of reliability test results

Category	Index combination	Alpha coefficient(α)
Patella prosthesis components	Number of units	0.7642
	Number of nodes	
	Material/density	
	Elastic modulus	
	Poisson's ratio	
Femoral prosthesis components	Number of units	0.8224
	Number of nodes	
	Material/density	
	Elastic modulus	
	Poisson's ratio	
Tibia prosthesis components	Number of units	0.8396
	Number of nodes	
	Material/density	
	Elastic modulus	
	Poisson's ratio	

It can be seen from Table 1 that the number of elements, number of nodes, material/density, elastic modulus, and poisson's ratio of the prosthetic components at each site have an acceptable impact on this experiment ($\alpha > 0.7$). Here we build a knee joint motion model based on the material properties of the components. This process plays a pivotal role in the entire experiment process, laying the foundation for the next step.

4.2. Finite Element Knee Joint Movement

(1) Apply 1200N compression force and 150N femoral posterior thrust

Here we first apply 1200N compression force and 150N femoral posterior thrust to the knee joint motion model built earlier, and collect the anterior-posterior (AP), medial and lateral (ML), internal and external rotation angles (IE), and varus angles (VV).), the results are shown in Table 2, and we make a bar graph based on this result, as shown in Figure 3.

Table 2. When a compression force of 1200N and a posterior femoral thrust of 150N are applied, the relative motion results of the tibiofemoral joint

Angle of flexion and extension	A-P(mm)	M-L(mm)	I-E(°)	V-V(°)
0 °	4.28	1.40	3.60	0.66
10 °	5.07	1.48	3.98	0.65
20 °	6.34	1.59	4.83	0.59
30 °	6.96	1.72	5.72	0.54
40 °	7.21	1.66	5.44	0.67
50 °	6.76	1.59	4.92	0.79
60 °	5.55	1.50	4.58	0.88

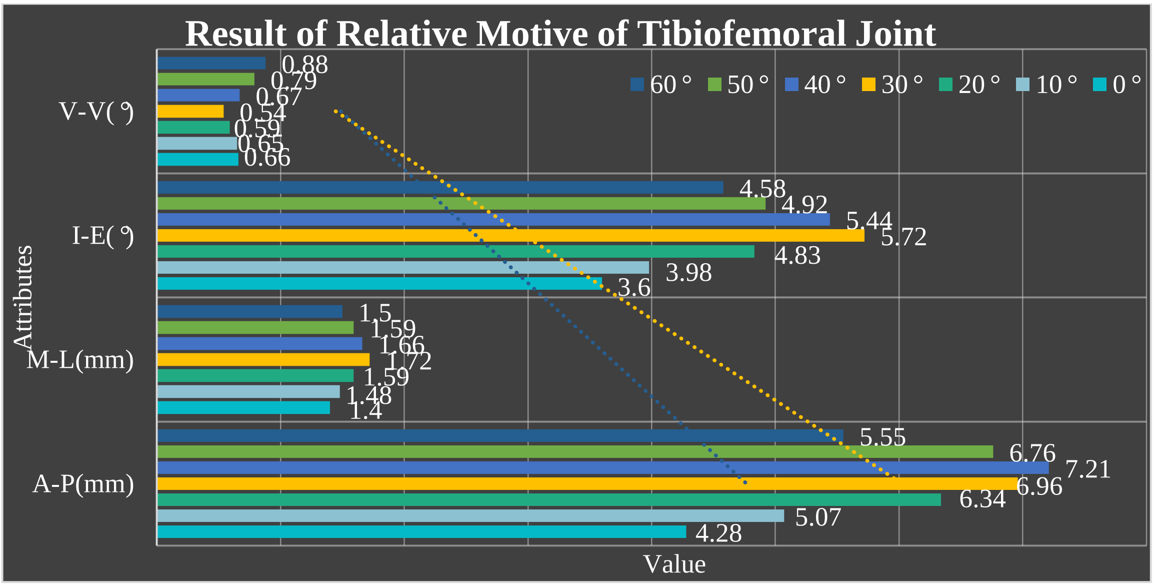

Figure 3. Results of relative motion of tibiofemoral joint

When the flexion and extension are 0 ° to 60 °, the compression force of 1200N and the femoral thrust force of 150N are applied, the relative displacement between the tibiofemoral joints is mainly the anterior and posterior displacement, and the minimum displacement is 4.28mm when the flexion and extension are 0 °; The maximum displacement is 6.96mm at 30 °. The relative displacement in other directions is small, and the rotation angle does not change much. The specific situation is shown in Figure 3.

(2) Apply 1200N compression force and 15Nm inversion and eversion moment

Here we first apply a compression force of 1200N and 15Nm of varus and valgus moments to the knee joint motion model built earlier, and collect the front and back direction (AP), the inner and outer direction (ML), the inner and outer rotation angle (IE), and the varus angle (VV) experimental data, the results are shown in Table 3. We make a combination diagram based on this result, as shown in Figure 4.

Table 3. The relative valgus angle of the tibiofemoral joint when a compression force of 1200N and a moment of varus and valgus of 15Nm are applied

Angle of flexion and extension	A-P(mm)	M-L(mm)	Inversion angle(°)	Eversion angle(°)
0 °	3.23	1.33	3.85	3.55
10 °	4.38	1.56	4.08	4.17
20 °	5.13	1.82	5.14	4.62
30 °	5.28	2.24	5.68	5.50
40 °	6.85	1.93	5.39	5.61
50 °	5.41	1.72	5.63	5.83
60 °	5.15	1.58	5.92	6.19

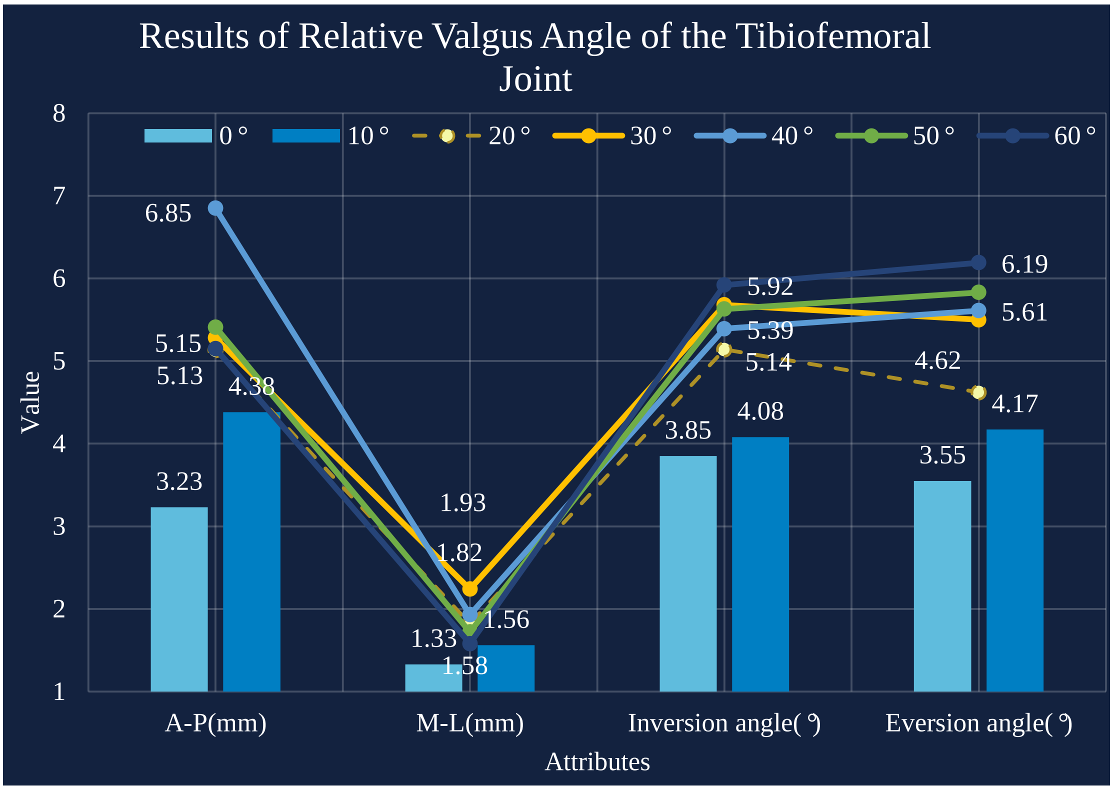

Figure 4. Results of the relative valgus angle of the tibiofemoral joint

Since it does not include muscles and skin tissues, 15Nm of varus and valgus moments are used, and the knee joint is in flexion and extension from 0 °to 60 °, and the range of movement of the knee joint is 3.55 °to 6.19 °. The movement is relatively stable and the angle changes little. The specific situation is shown in Figure 4.

(3) Apply 1200N compression force and 8Nm internal and external rotation torque

Here we first apply a compression force of 1200N and an internal and external rotation torque of 8Nm to the previously built knee joint motion model, and collect the front-rear direction (AP), the internal-external direction (ML), the internal-external rotation angle (IE) and the varus angle (VV) experimental data, the results are shown in Table 4, we make a histogram based on this result, as shown in Figure 5.

Table 4. When a compression force of 1200N and a torque of 8Nm internal and external rotation are applied, the relative internal rotation angle of the tibiofemoral joint

Angle of flexion and extension	A-P(mm)	M-L(mm)	Pronation angle(°)	External angle(°)
0°	2.03	2.24	2.25	1.75
10°	2.4	2.87	11.32	9.36
20°	3.34	3.15	20.56	22.28
30°	4.06	4.38	24.65	28.52
40°	5.47	4.92	25.37	29.83
50°	5.3	4.87	27.63	30.77
60°	7.27	6.86	29.34	33.34

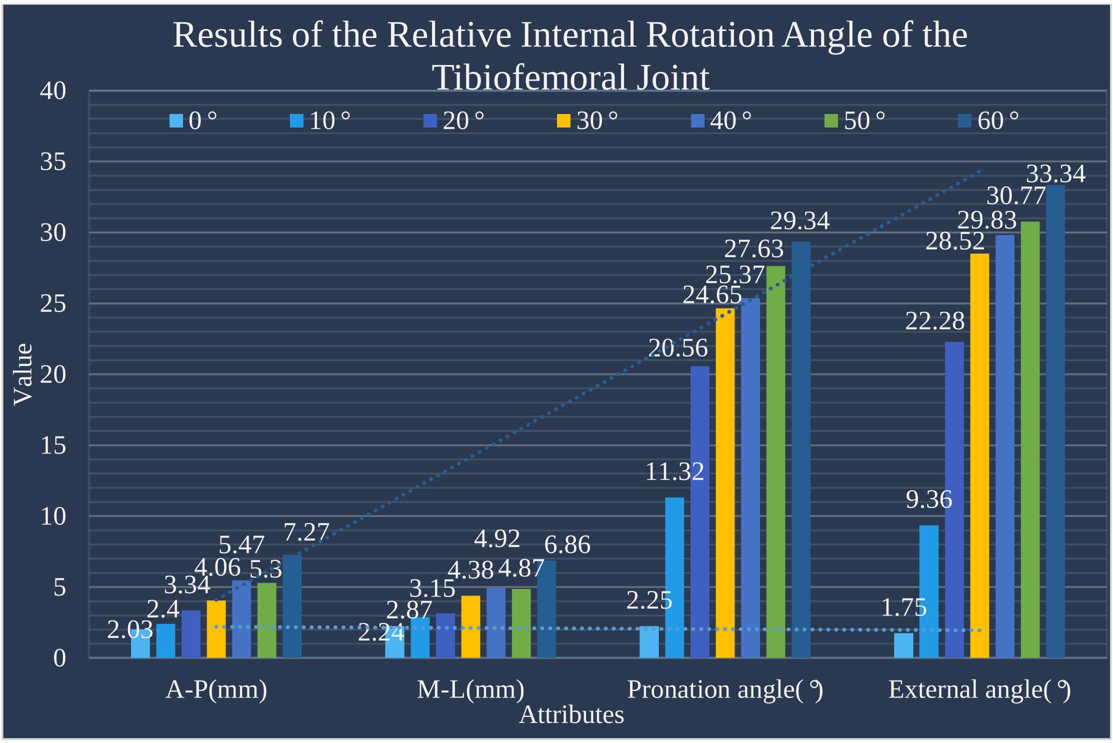

Figure 5. Results of the relative internal rotation angle of the tibiofemoral joint

Applying a compression force of 1200N while using a torque of 8Nm internal rotation, it was measured that the range of internal rotation of the knee joint was 2.25° to 29.34° and the range of external rotation was 1.75° to 33.34° during knee flexion from 0° to 60°. It can be seen that the angles of internal and external rotation gradually increase with the increase of flexion and extension, but the range of external rotation is slightly larger than the range of internal rotation. The specific situation is shown in Figure 5.

4.3. Finite Element Settlement Results

The establishment of a mechanical model has its limitations and cannot fully express all the biomechanical properties of cartilage. Therefore, the obtained results and experimental data will have certain deviations. The results are shown in Table 5. We make a doughnut chart based on this result, as shown in Figure 6.

Table 5. Stress-velocity data for cartilage compression test

$\sigma(Kpa)$	10	20	30	40	50	60	70
$v(\mu m/s)$	0.987	0.972	0.964	0.953	0.947	0.910	0.895
$\sigma(Kpa)$	80	90	100	110	120	130	140
$v(\mu m/s)$	0.873	0.852	0.809	0.782	0.713	0.662	0.659
$\sigma(Kpa)$	150	160	170	180	190	200	-
$v(\mu m/s)$	0.529	0.476	0.395	0.290	0.062	0.041	-

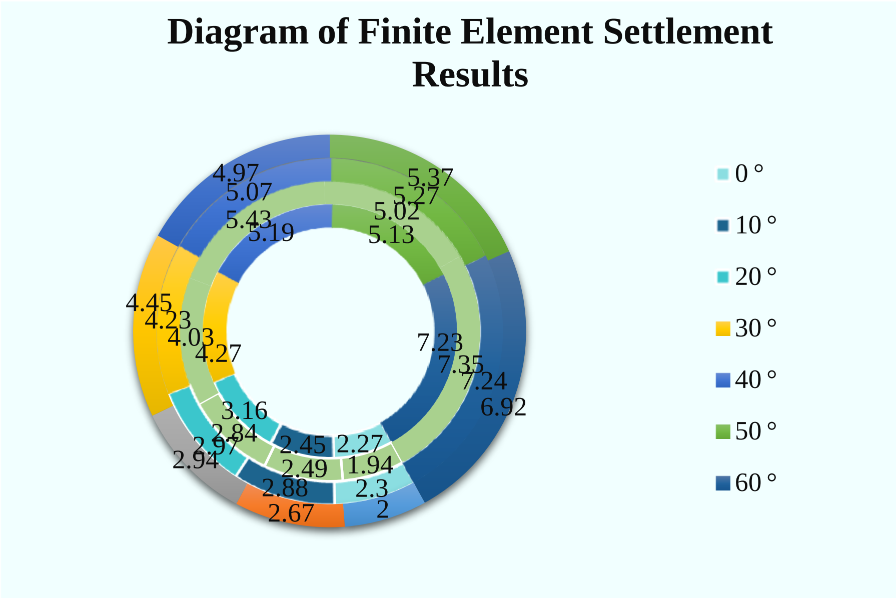

Figure 6. Analysis diagram of finite element settlement results

It can be seen from Figure 6 that as the stress continues to increase, the value of the velocity shows a decreasing trend, when the pressure on the cartilage surface increases, the ability of the cartilage to resist external forces is also increasing, and the rate of deformation gradually decrease. The overall trend of the three sets of data relationship curves is roughly the same. At the initial stage of loading, the stress and speed results obtained from the three sets of data have a small difference, and there are certain differences in the curves as the stress increases.

4.4. Gait Simulation

The knee joint after replacement is applied with the same load as the gait motion of the natural knee joint, and the gait motion of the knee joint is simulated, and the relative motion and mechanical characteristics of the artificial joint during the gait process are studied and analyzed. The results are shown in Table 6. We make a bar graph based on this result, as shown in Figure 7.

In the gait movement of the knee joint after simulated replacement, the medial and lateral displacement of the tibiofemoral joint and the angle of varus and valgus are relatively stable; the range of the posterior movement of the tibiofemoral joint during gait is 0.56mm to 4.39mm. Around 20% and 60% of the gait are two maximum points, 4.20mm and 4.39mm respectively. The angle of internal and external rotation is relatively stable from 0% to 40%, and the angle of internal and external rotation gradually increases from 40% to 90%, reaching a maximum of 5.45 °around 90%.

Table 6. The result of the relative movement of the tibiofemoral joint during gait

Gait cycle	A-P(mm)	M-L(mm)	I-E(°)	V-V(°)
0°	0.55	1.03	0.52	0.43
10°	5.07	1.19	0.68	0.55
20°	4.20	1.36	0.97	0.68
30°	1.62	1.28	0.64	0.62
40°	0.77	1.21	0.50	0.55
50°	1.94	1.37	1.43	0.64
60°	4.39	1.47	2.01	0.72
70°	3.12	1.56	3.21	0.75
80°	2.41	1.62	4.38	0.80
90°	1.26	1.70	5.45	0.85

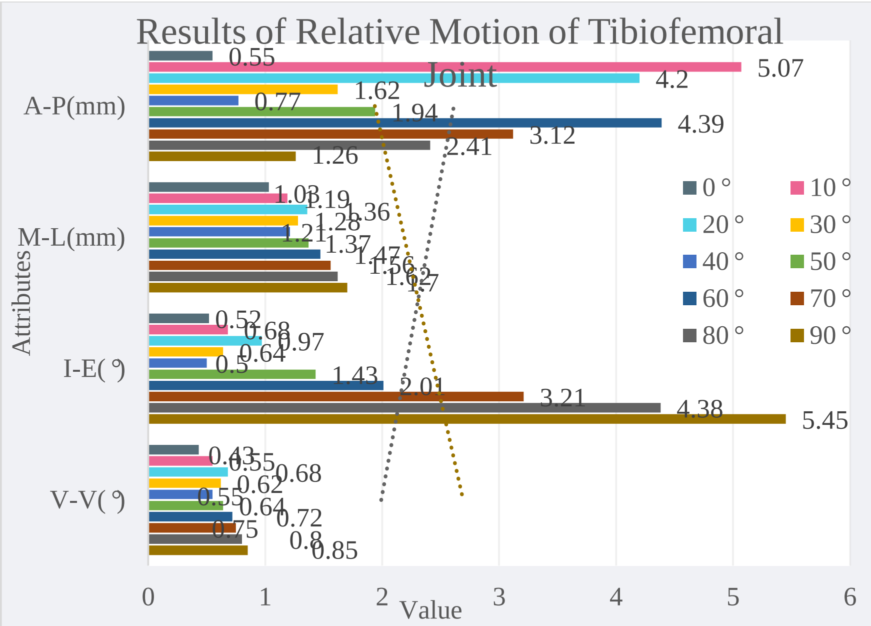

Figure 7. Results of relative motion of tibiofemoral joint

5. Conclusion

The finite element method can overcome some shortcomings in traditional research. Its biggest disadvantage is that it cannot analyze the mechanical properties of joints with complex geometric structures. In the biomechanics research of the knee joint, the three-dimensional finite element model can more accurately simulate the various movements of the knee joint in daily life, and can obtain the motion status and biomechanical characteristics of the knee joint under complex conditions. For now, most of the knee joint models have not been able to assemble the various structures of the knee joint, some lack the meniscus, and some ligaments are incomplete; and the finite element analysis of the knee joint is mostly static simulation. Therefore, there is a big gap between the experimental results obtained and the actual situation. In this paper, a complete three-dimensional finite element model of the knee joint including bones, ligaments, all cartilage and meniscus was built, and compared with other people's experiments. Although there are some differences, most of the results are consistent with the data, which can prove the effectiveness of this model.

Based on the microscopic structural properties and macroscopic mechanical properties of articular cartilage, this paper establishes a two-phase porous medium superelastic model of cartilage, which is used to simulate the biomechanical properties of articular cartilage, and then based on the control equation that can express the mechanical properties of cartilage. The nonlinear system balance equation is established and numerically solved. Finally, the analysis results obtained by the finite element solution are compared with the experimental results of known references to verify the model. When simulating natural knee flexion from 0° to 60°, the internal rotation angle and the valgus angle gradually increase with the increase of the flexion and extension angle, and the internal rotation angle changes greatly, ranging from 0° to 30°, while the valgus angle changes it is relatively small, ranging from 3.60° to 5.72°; the femur has a significant posterior shift relative to the tibia, ranging from 4.28mm to 7.21mm, and the medial and lateral displacements are relatively stable.

Through the finite element numerical simulation, the stress-strain relationship curve of the nonlinear exponential relationship of the articular cartilage is obtained. By comparing with the stress-strain curve in the experiment, it can be found that the data obtained by the model is basically consistent with the experimental data, the error is small, and it can be compared. It truly reflects the stress-strain relationship of biological tissue under load; through numerical simulation of cartilage compression experiment, the velocity-stress relationship curve of articular cartilage is obtained, and the data on the velocity-stress relationship curve is compared with theories in other literatures comparing the data, it can be found that the data result has been optimized. Comparing it with the known experimental data, the accuracy of the finite element calculation result is verified. At the same time, there are some shortcomings in this article that need to be improved and deepened. Due to time constraints, the finite element analysis of the equation is only an iterative operation within a time step to obtain the deformation process obtained by applying the load in this instant. Next, it is necessary to obtain the deformation analysis in the entire time domain.

Funding

This article is not supported by any foundation.

Data Availability

Data sharing is not applicable to this article as no new data were created or analysed in this study.

Conflict of Interest

The author states that this article has no conflict of interest.

References

[1] Mika J, Clanton T O, Ambrose C G, et al. Surgical Preparation for Articular Cartilage Regeneration in the Osteoarthritic Knee Joint. Cartilage. (2017) 8(4): 365-368. https://doi.org/10.1177/1947603516670710

[2] Pame M, Gayan M, Hazarika K, et al. Mri Evaluation of Painful Knee Joint- The Correlation of Multiple Coexisting Pathologies, Age and Sex. Journal of Evidence Based Medicine and Healthcare. (2017) 4(18): 1019-1027. https://doi.org/10.18410/jebmh/2017/200

[3] Hoekstra M, Veltman E S, Nurmohamed R F R H A, et al. Sonication Leads to Clinically Relevant Changes in Treatment of Periprosthetic Hip or Knee Joint Infection. Journal of Bone and Joint Infection. (2020) 5(3): 128-132. https://doi.org/10.7150/jbji.45006
[4] Tseng F J, Lin G J, Chen Y W, et al. Knee Joint Injection Resveratrol Amelioration Inflammation in Collagen Antibody Induced Arthritis. Journal of Medical ences. (2019) 39(5): 223-230. https://doi.org/10.4103/jmedsci.jmedsci_8_19
[5] Skvortsov D V, Churkin S N, Akhpashev A A, et al. Biomechanics of walking before and after surgical treatment of damaged menisci of the knee joint. Rheumatology ence and Practice. (2019) 57(1):106-110. https://doi.org/10.14412/1995-4484-2019-106-110
[6] Prlkov-Pukov A, Touraov A, Vali P, et al. Reliability of the Evaluation of MRI Examinations after the Treatment of Chondral Defects in the Knee Joint. Acta chirurgiae orthopaedicae et traumatologiae Cechoslovaca. (2020) 87(4): 251-258.
[7] A K B S, C T A B, D T E F, et al. Assessment of objective dynamic knee joint control in anterior cruciate ligament deficient and reconstructed individuals. The Knee. (2019) 26(3):578-585. https://doi.org/10.1016/j.knee.2019.02.013
[8] Zhang J, Song G Y, Feng H. Development of heterotopic ossification after multiple-ligament reconstruction of the knee joint: Incidence and explanatory factor analysis. The Knee. (2020) 27(3): 642-648. https://doi.org/10.1016/j.knee.2020.04.012
[9] Yang Z Q. Research status of knee joint replacement. Zhongguo gu shang = China journal of orthopaedics and traumatology. (2020) 33(1): 1-3.
[10] Alouane M A, Rifai H, Kim K, et al. Hybrid impedance control of a knee joint orthosis. Industrial Robot. (2019) 46(2): 192-201. https://doi.org/10.1108/IR-08-2018-0165
[11] Fukaya T, Mutsuzaki H, Mori K. Relations between external moment and movement of the knee joint during the stance phase in patients with severe knee osteoarthritis. Journal of Orthopaedics. (2019) 16(1): 101-104. https://doi.org/10.1016/j.jor.2018.12.014
[12] Street B D, Gage W. Younger Total Knee Replacement Patients Do Not Demonstrate Gait Asymmetry for Heel Strike Transient or Knee Joint Moments That Are Observed in Older Patients. Journal of Applied Biomechanics. (2019) 35(2): 140-148. https://doi.org/10.1123/jab.2018-0120
[13] Thomas T M, Candrea D N, Fifer M S, et al. Decoding Native Cortical Representations for Flexion and Extension at Upper Limb Joints Using Electrocorticography. IEEE Transactions on Neural Systems and Rehabilitation Engineering. (2019) 27(2): 293-303. https://doi.org/10.1109/TNSRE.2019.2891362
[14] Daniels J, Phillips K L, Chiverton N, et al. Phrenic Nerve Transfer for Reconstruction of Elbow Extension in Severe Brachial Plexus Injuries. Journal of Reconstructive Microsurgery. (2016) 32(07): 546-550. https://doi.org/10.1055/s-0036-1583302
[15] Namazi H, Kayedi T. Investigating the Effect of Intra-articular Platelet-Rich Plasma Injection on Union: Pain and Function Improvement in Patients with Scaphoid Fracture. J Hand Microsurg. (2016) 08(03): 140-144. https://doi.org/10.1055/s-0036-1597088
[16] Arias S, Rogeli P, Garay L, et al. A System for Simultaneous Finger Joints Goniometric Measurements Based on Inertial Sensors. IEEE Latin America Transactions. (2017) 15(10): 1821-1826. https://doi.org/10.1109/TLA.2017.8071222
[17] Iglesias M, Salazar-Hernández, Fernanda, Ramírez-Berumen, María, et al. Anatomical and Microsurgical Implications in Total and Midarm Transplantation. Journal of Reconstructive Microsurgery Open. (2017) 02(02): e94-e102. https://doi.org/10.1055/s-0037-1604342
[18] Bersini S, Sansone V, Frigo C A. A dynamic multibody model of the physiological knee to predict internal loads during movement in gravitational field. Computer Methods in

Biomechanics & Biomedical Engineering. (2016) 19(5-8): 571-579. https://doi.org/10.1080/10255842.2015.1051972

[19] Chen X, Delp S L. Human soleus sarcomere lengths measured using in vivo microendoscopy at two ankle flexion angles. Journal of Biomechanics. (2016) 49(16): 4164-4167. https://doi.org/10.1016/j.jbiomech.2016.11.010

[20] Chang-Sun, Kim, Sang-Jin, et al. Evaluation of Muscle Strength Laterality in Korean Traditional Archers. Journal of the Korean Society of Living Environmental System. (2017) 24(3): 343-350. https://doi.org/10.21086/ksles.2017.06.24.3.343

[21] Huang P C, Pande P, Ahmad A. Magnetomotive Optical Coherence Elastography for Magnetic Hyperthermia Dosimetry Based on Dynamic Tissue Biomechanics. IEEE Journal of Selected Topics in Quantum Electronics. (2016) 22(4): 104-119. https://doi.org/10.1109/JSTQE.2015.2505147